<Technical Report>

Operational Application of Meteorology and Climate Monitoring in the Tropics[1]

Atsushi Goto
Tokyo Climate Center, Climate Prediction Division
Global Environment and Marine Department
Japan Meteorological Agency

Contents

[1] Short-term Expert training course 2, JICA-Sri Lanka Department of Meteorology Improving of Meteorological Observation, Weather Forecasting & Dissemination Project, 23-27 January 2017

Some parts of this lecture note, especially its chapter 3, are quoted from the textbook “The Asian monsoon”. From a view point of copyright protection, no part of this note may be made available to unspecified third parties, reproduced and redistributed in any manners. Any mistakes in this note are my own.

Contact: atsushi.goto@met.kishou.go.jp

1. Introduction: Importance of understanding of climatological normals in atmospheric circulation

The term ‘monsoon’ stems from seasonal variations in winds but it is now more generally applied to tropical and subtropical seasonal reversals in both the atmospheric circulation and associated precipitation. The climate of the tropical Indian Ocean region including Sri Lanka is dominated by the Indian monsoon and therefore the atmospheric circulation shows significant seasonal change. When considering weather forecasts or causes of anomalous climate events, some forecasters are prone to focus only on and discuss anomalies of atmospheric circulation. However, as you are already aware, this is not appropriate approach particularly in the region where atmospheric circulation varies as season.

Let’s think this point through an example. Figure 1.1 shows the monthly mean wind anomaly at 850 hPa level for a certain month. Hereafter in this note, the term “normal” means the 30-year average from 1981 to 2010 and the term “anomaly” means the deviation from “normal”.

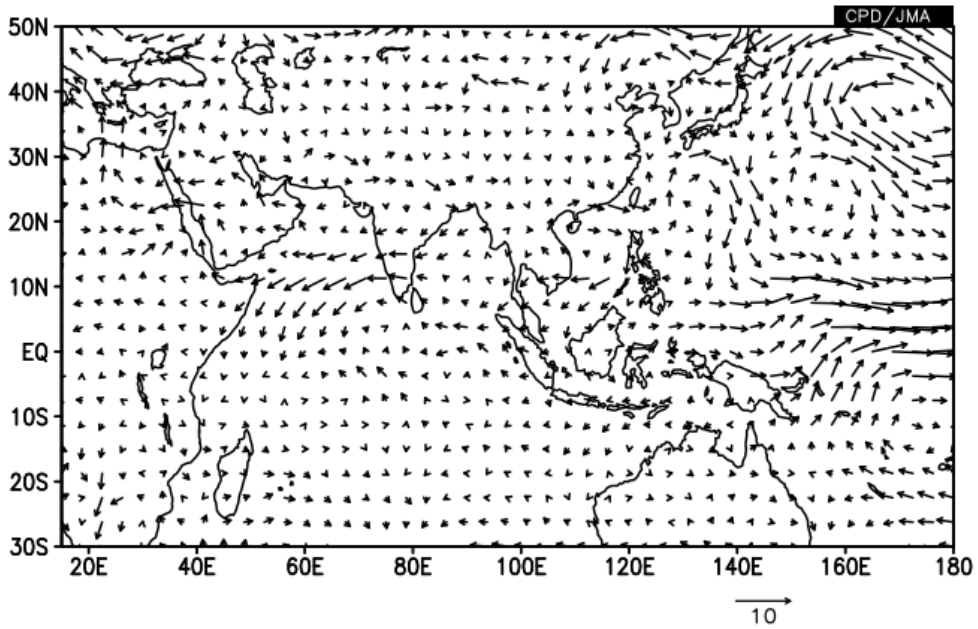

Figure 1.1 The monthly mean wind anomaly at 850 hPa level for a certain month.

A unit of reference wind vector is [m/s].

Exercise 1.1

Which description is the most reasonable for the interpretation of Figure 1.1?

a) This figure indicates weaker southwesterly monsoon and it is likely to be drier condition in Sri Lanka.

b) This figure indicates stronger northeasterly monsoon and it is likely to be wetter condition in northeastern Sri Lanka.

c) It cannot be determined by this figure alone.

If you select c), please describe which kind of information is necessary for appropriate interpretation.

Exercise 1.2

Figure 1.2 shows the normal of monthly mean wind at 850 hPa level for August. Given Figure 1.1 shows the monthly mean wind anomaly at 850 hPa level for August 2015, which description of Exercise 1.1 is the most reasonable for the interpretation?

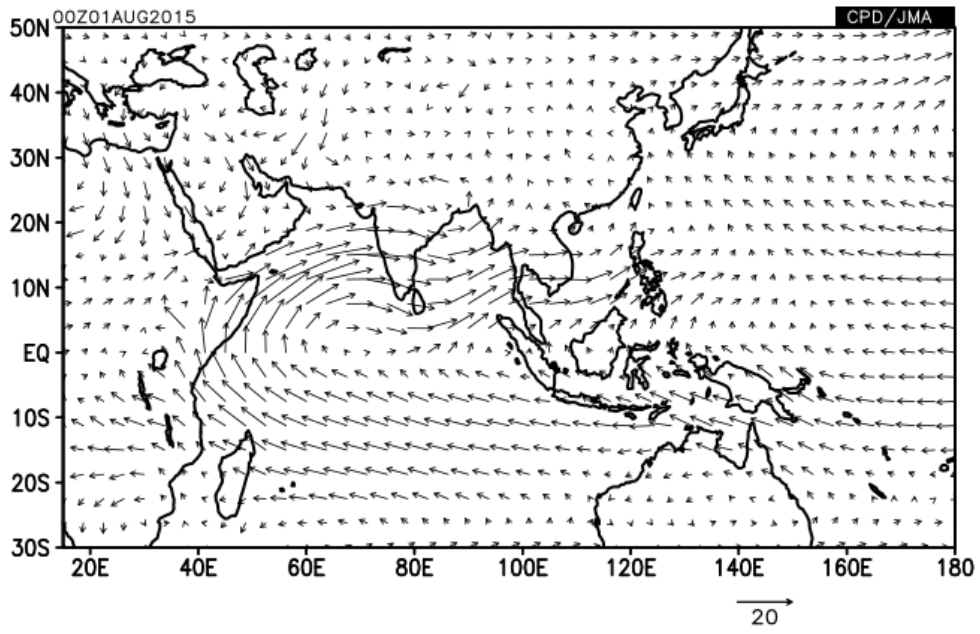

Figure 1.2 The normal of monthly mean wind at 850 hPa level for August.

A unit of reference wind vector is [m/s].

These two exercises clearly tell that the information about when is necessary, however, it is not sufficient unless we don't comprehend the basic state, in other words "normal" of climate at the time. The understanding of climatological normals in atmospheric circulation helps us to monitor and understand the current climate systems and furthermore, helps to obtain a deeper insight from results of climatological

researches, such as a statistical investigation between ENSO and local climate. Let's think this point through the next example.

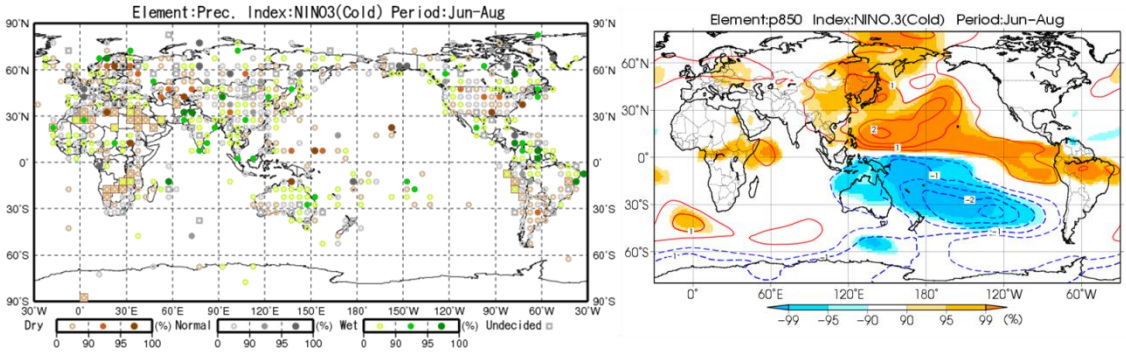

Figure 1.3 Anomalies of precipitation (left) and stream function at 850 hPa level (right) appeared in the past La Niña events for June-August mean.

Figure 1.3 is a result of statistical investigation regarding ENSO and local climate or atmospheric circulation conducted by the Tokyo Climate Center of the Japan Meteorological Agency. Full results of these investigations are available from below web pages of the TCC website.

- Impact on climate: http://ds.data.jma.go.jp/gmd/tcc/tcc/products/climate/ENSO/month.html
- Impact on atmospheric circulation: http://ds.data.jma.go.jp/gmd/tcc/tcc/products/clisys/enso_statistics/index.html

Exercise 1.3

Under La Niña conditions,

(1) Which is it likely to be drier or wetter over Sri Lanka and southern India?

(2) Which is it likely to appear a clockwise or anticlockwise circulation anomaly at lower troposphere over the tropical Indian Ocean? (Please note that positive stream function indicates a clockwise circulation.)

Then,

(3) Please explain the relationship between answers of (1) and (2) by reference to Figure 1.2.

This course aims to visualize the "normal" condition of atmospheric circulation for each month by using TCC's Interactive Tool for Analysis of Climate System "iTacs", and understand its structure and mechanism from a meteorological perspective in order to build the ground of improved climate monitoring and analysis.

2. Basic climate variables

Monsoons are a response of the coupled atmosphere-ocean-land system to annual variation of solar radiation forcing. Physical processes governing monsoon climate involve not only atmospheric dynamical processes but also extremely complex interaction among the atmosphere, ocean, and land surface processes. The seasonal changes in atmospheric circulation in monsoon region arise from reversals in heating and temperature gradients between continental regions and the adjacent oceans with the progression of the seasons.

In the sea level pressure field, the main features are the subtropical anticyclones that are strongest in the summer hemisphere and extend to higher latitude in the northern summer. However, the oceanic anticyclones in northern summer over the Pacific and Atlantic are also strong persistent features directly linked to regional monsoon circulation. Tropic continents are regions of low pressure, often as part of the monsoon trough.

In the lower troposphere, the equatorial trough in the boreal winter, the major monsoon trough over Asia in the boreal summer, the subtropical anticyclones with strong southeast and northeast trade winds, and the higher latitude westerlies are all notable features.

Though the dominant flow is the rotational component (shown by the stream function) that is largely related to the monsoon circulation, of more interest with respect to monsoons is the divergent part of the flow itself, shown with the velocity potential as a much smoothed depiction of the global-scale divergent field. As low-level convergence at 850hPa is generally manifested as upper level divergence at 200hPa, these fields strongly indicate the large-scale monsoonal overturning circulations.

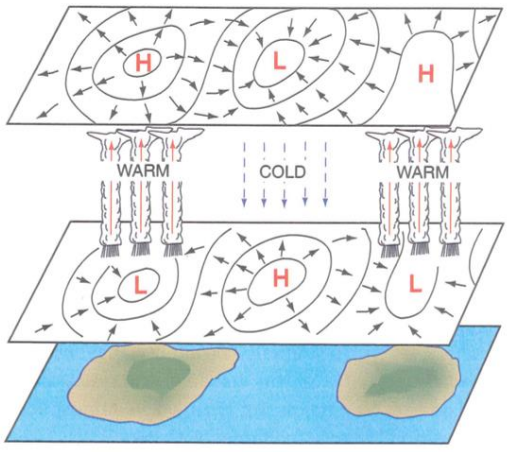

Figure 2.1
Idealized representation of monsoon circulations.
The islands represent the subtropical continents in the summer hemisphere (quoted from Fig. 10.9 of “Atmospheric Science” by John M. Wallace).

Exercise 2.1

A description in the previous page is quoted from a textbook “The Asian Monsoon” (edited by Professor Bin Wang) to illustrate the basic feature of monsoons. Referring to above description (especially underlined parts), please give a set of variables necessary to depict features of monsoon as many as possible, together with for what feature you depict.

Variables	Level	For what
ex) net solar radiation	TOA	To understand the seasonal variation of solar radiation forcing

Exercise 2.2

Draw maps of monthly-averaged climatological normals of variables listed in Exercise 2.1 for each month using TCC’s “iTacs”.

3. Understanding of climatological normals in atmospheric circulation

In this chapter, we will review the seasonal variation of monsoon circulation through both figures of climatological normal and explanatory descriptions. Description of this chapter is based on the textbook "The Asian monsoon" (Wong, 2006).

3.1 Radiative forcing as a driving force of monsoon

The fundamental forcing of the atmospheric circulation and climate ultimately relates to the radiation budget of the planet. To further set the stage for understanding the seasonal monsoon variations, we therefore examine the diabatic forcing of the atmospheric circulation.

The dominant annual cycle forcing is the change in distribution of incoming solar radiation due to the orbit of the Earth around the sun (Figure 3.1). There important effects from albedo and clouds, but they are secondary and the pattern of net solar radiation at the top of the atmosphere has a strong zonal component that is dominated by orbital effects. On the other hand, the outgoing longwave radiation (OLR) is more uniform with latitude and seasons, and is well established to vary primarily with deep convection, owing to the high cold cloud tops (Figure 3.2). The cloud signature in the net solar radiation at the top of the atmosphere is well matched by that in the OLR signal, however, the net radiation seasonally is dominated by the net solar radiation changes and the zero line in the net radiation (not shown) lies just north of the equator. It is this pattern of net radiation that ultimately directly drives the monsoons and their seasonal reversals.

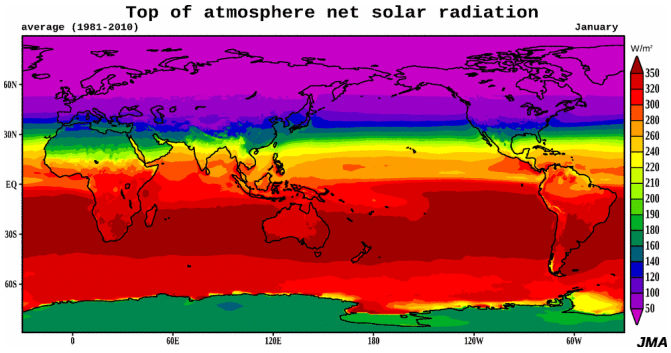

(January)

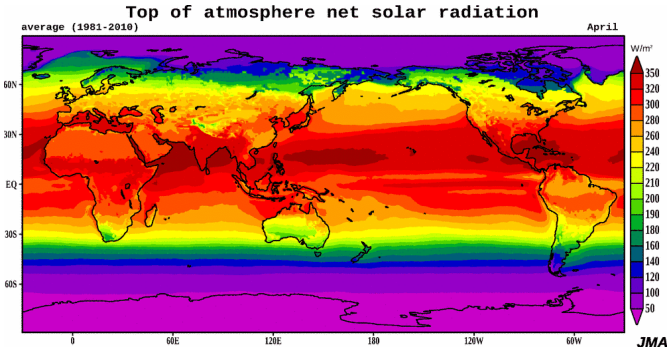

(April)

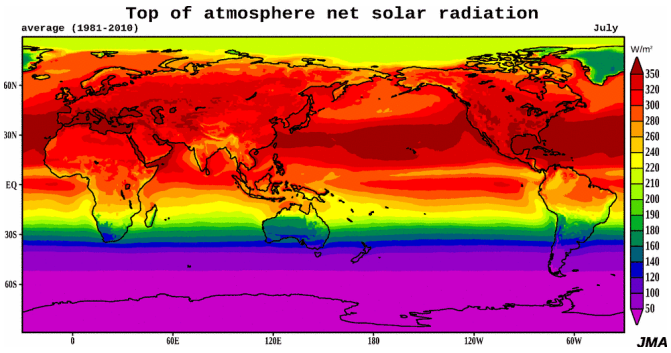

(July)

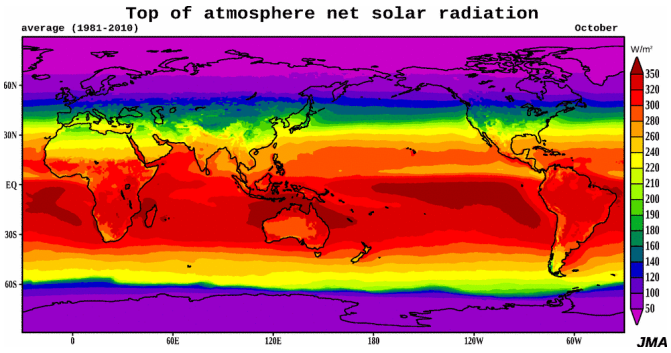

(October)

Figure 3.1 Monthly mean net solar radiation at the top of the atmosphere (estimation in JMA's long-term reanalysis data JRA-55, unit: W/m^2).

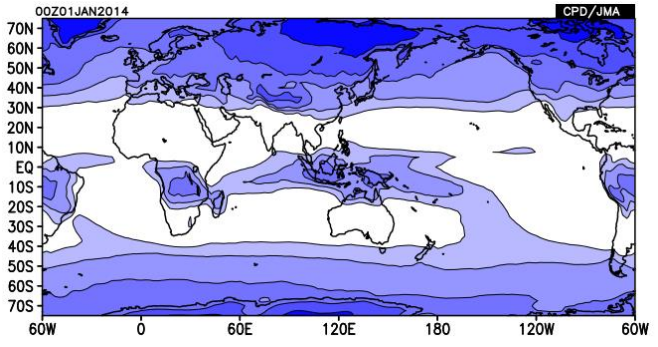

(January)

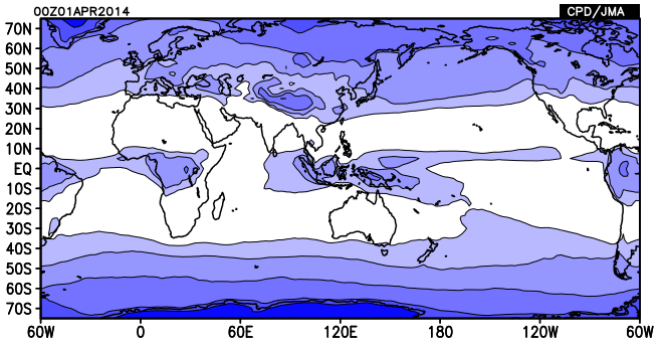

(April)

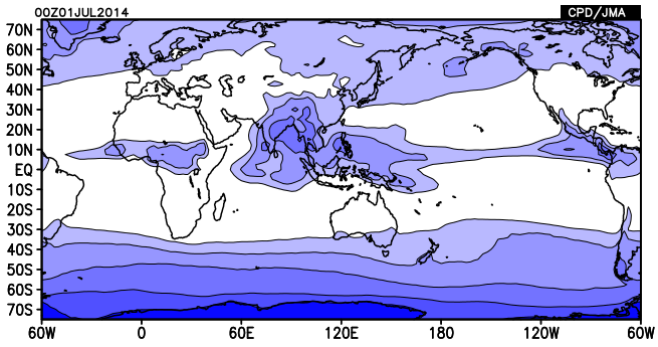

(July)

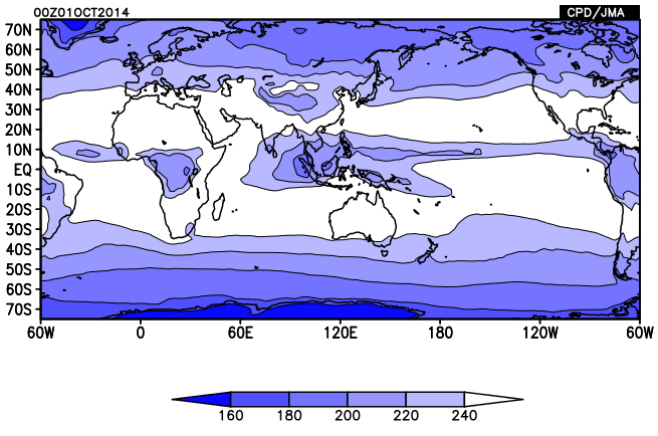

(October)

Figure 3.2 Monthly mean outgoing long-wave radiation (OLR) (unit: W/m^2).

3.2 Onset of a summer monsoon

One of the critical aspects of monsoon cycle is the reversing cross-equatorial, low-level atmospheric flow. This flow results from an oscillating cross-equatorial pressure gradient. During summer a planetary-scale warm air mass is centered on south Asia with the maximum average layer temperature over the southern Tibetan Plateau, resulting in strong temperature gradients in both the north-south and east-west direction. The reversal of the meridional temperature gradient occurs first on the south side of the Tibetan Plateau (near 90-100E) and then expand over the large area extending from Africa to the western Pacific (Figure 3.3). Li and Yanai (1996) found that the onset of the Asian summer monsoon is concurrent with the reversal of meridional temperature gradient in the upper troposphere south of the Tibetan Plateau (Figure 3.4). Geostrophic adjustment to the elevated heating over the Himalayas is sufficiently rapid to allow the development of a substantial pressure field and a warm core.

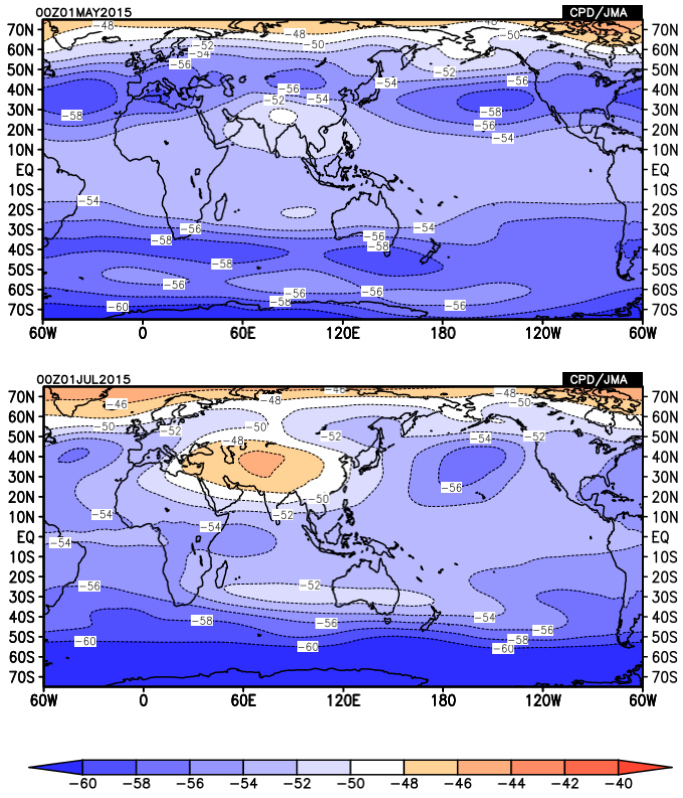

Figure 3.3 Monthly mean air temperature at 200 hPa level (unit: degree C).

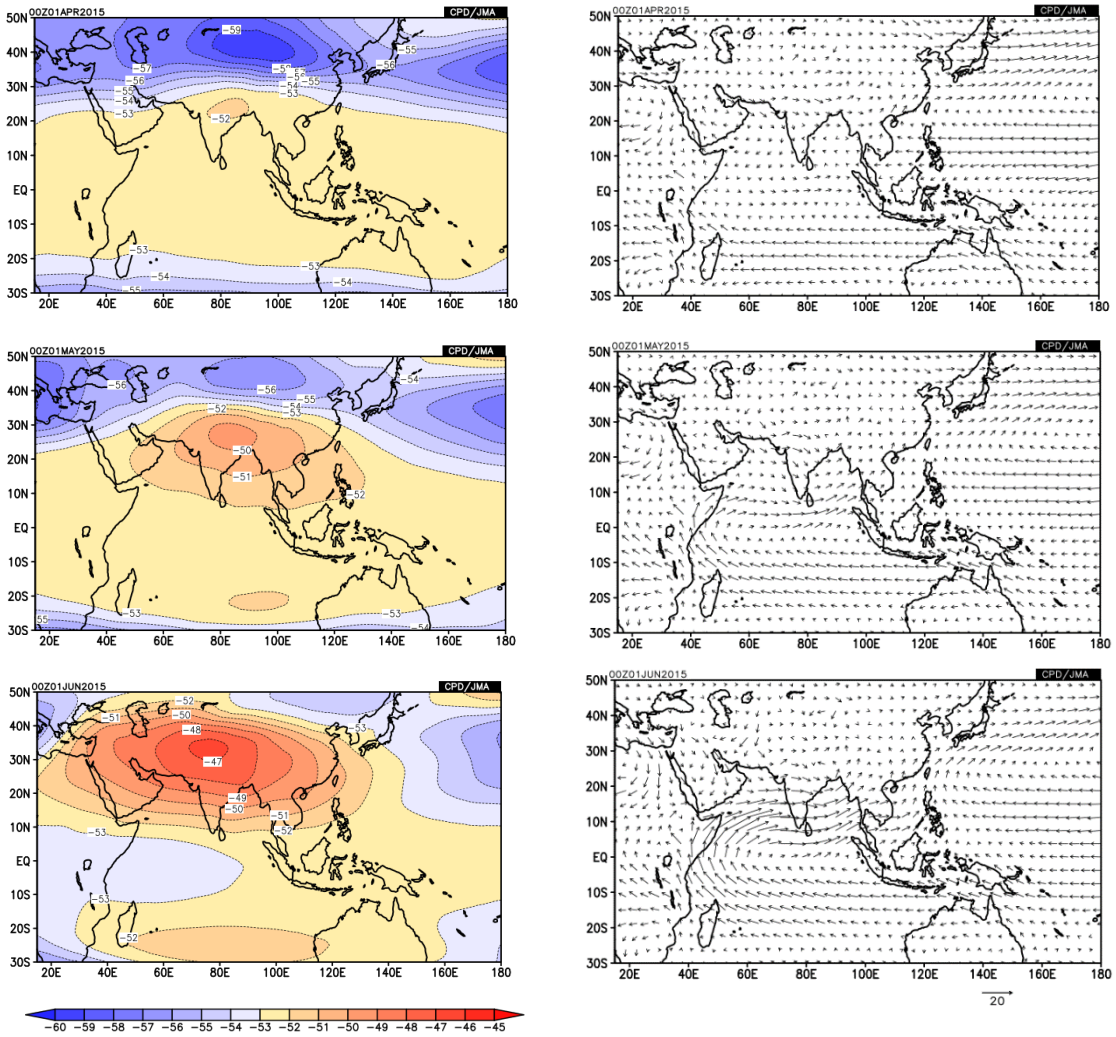

Figure 3.4 Monthly mean air temperature at 200 hPa level (left, unit: degree C) and wind at 850 hPa level (right, unit: m/s) for April (top), May (middle) and June (bottom).

The monsoon is manifested as a land-atmosphere-ocean interaction between continent and oceans in the seasonal cycle. The ocean has a large heat content with a longer climate memory of more than a year, but the land has a small heat content and its climate memory is believed to be short (less than a season). The land shows strong and rapid heating (and cooling) in the seasonal cycle which in turn has a large impact in seasonal atmospheric differential heating (and cooling) processes between the land and the ocean. Seasonal land surface heating and the resultant atmospheric heating over Eurasia manifests itself in the surface or lower tropospheric pressure field.

The large decrease of pressure over Eurasia is indicative of the seasonal heating of land, presumably centered over the Tibetan Plateau and Mongolia. The low-pressure area over southern Eurasia (called the ‘monsoon trough’) at the surface and lower troposphere induces moist south-westerly wind from the Indian

Ocean (the south-west monsoon flow) toward India, southeast Asia and east Asia, and dry northerly wind from the interior of the Eurasian continent (Figure 3.5). The moist monsoon flow, in turn, induces convection and precipitation over the south-eastern part of the continent, which plays a dominant role in atmospheric latent heating as a 'moist land-atmosphere interaction' during the monsoon season.

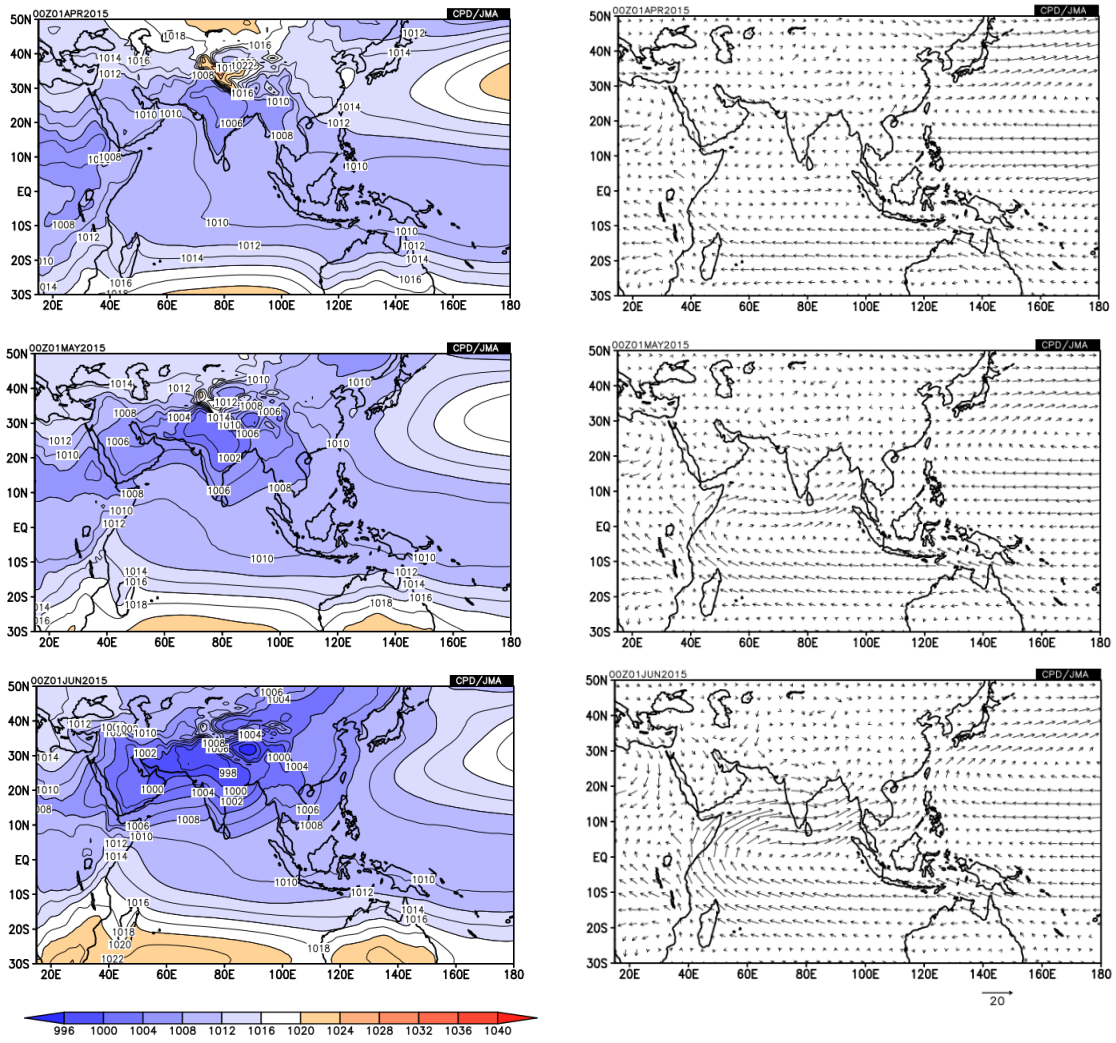

Figure 3.5 Monthly mean sea level pressure (SLP) (left, unit: hPa) and wind at 850 hPa level (right, unit: m/s) for April (top), May (middle) and June (bottom).

An important issue may be how this moist land-atmosphere interaction starts in the interior of the continent. Over the elevated land surface of the Tibetan Plateau, sensible heating plays a dominant role in atmospheric diabatic heating of the whole troposphere through deep, dry convection, particularly in the onset phase of the Asian monsoon. Diabatic heating over the Tibetan Plateau in the pre-monsoon phase causes horizontal temperature (pressure) gradients in the upper (lower) troposphere between the surrounding Indian and Pacific Oceans and the interior of the continent.

3.3 Dynamics of summer monsoon circulation

Figures 3.6 show OLR and the atmospheric circulation in the lower and upper troposphere in August, for matured summer monsoon circulation.

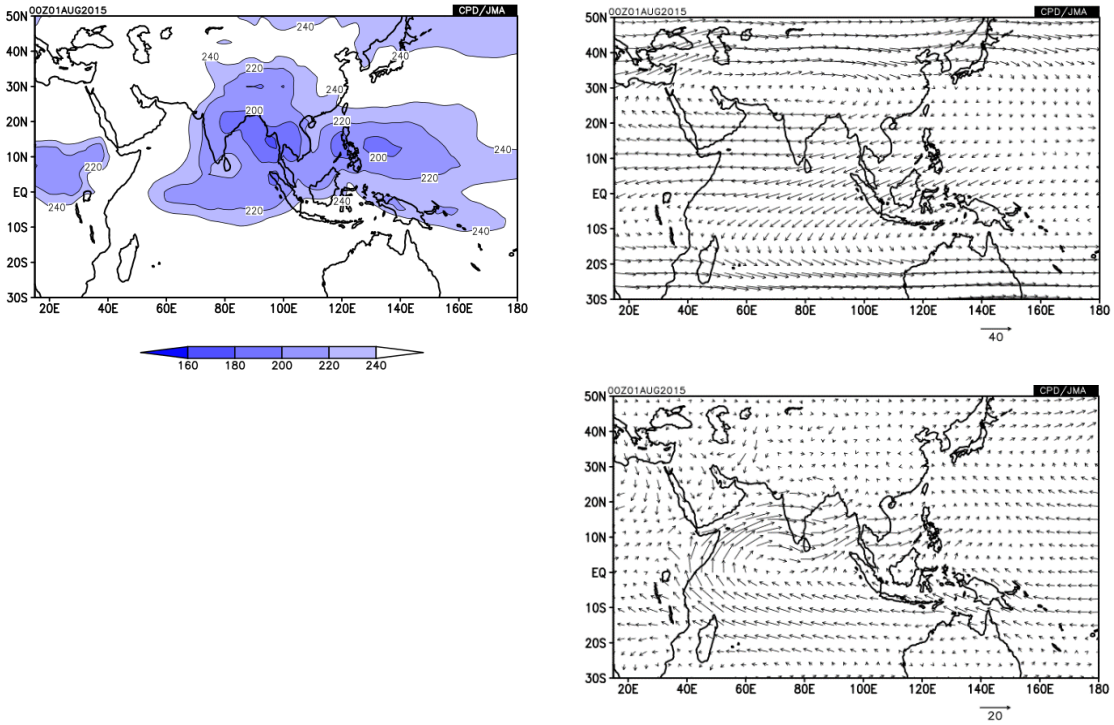

Figure 3.6 Monthly mean OLR (left, unit: W/m^2), wind at 200 hPa (top-right) and wind at 850 hPa level (bottom-right, unit: m/s) for August.

Exercise 3.1

Please illustrate features of convective activities and atmospheric circulation as detailed as possible. In this subsection we try to interpret and explain these features from a perspective of meteorology.

The dominant diabatic heating in the tropics comes from latent heating associated with precipitation. The heating is associated with regions of upward motion and the low-level convergence of moisture by the atmospheric circulation itself. The atmospheric circulation naturally responds to these diabatic forcing and, at the same time, transport the heat, energy, and moisture. The low-frequency part of the flow plays a dominant role throughout the tropics.

To the lowest order, the large-scale tropospheric motion stimulated by deep convective heating can be described by the lowest baroclinic mode for which the internal gravity wave speed for the dry atmosphere is C_0 = 50 m/s. The two parameters, $\beta$and C_0, which reflect the Earth's rotational and gravitational effects,

respectively, determine an equatorial trapped length scale $Rc = \sqrt{C_O/\beta}$ called the equatorial Rossby radius of deformation. A value of C_0 = 50 m/s corresponds to an equatorial Rossby radius of deformation of about 15 degrees of latitude.

To illustrate the fundamental physical processes, Gill (1980) used a single sinusoidal vertical mode, shallow-water equation model on an equatorial β-plane. This simplification is based on the consideration that the heating released in the middle troposphere stimulate primarily the lowest baroclinic vertical mode. Gill considered a steady-state motion in a resting basic state forced by a given heating Q. The forced motion is sufficiently weak that it can be treated using linear dynamics. The long-wave approximation is also taken (i.e., neglecting the high-frequency inertia-gravity waves, Rossby-gravity waves, and the short Rossby waves).

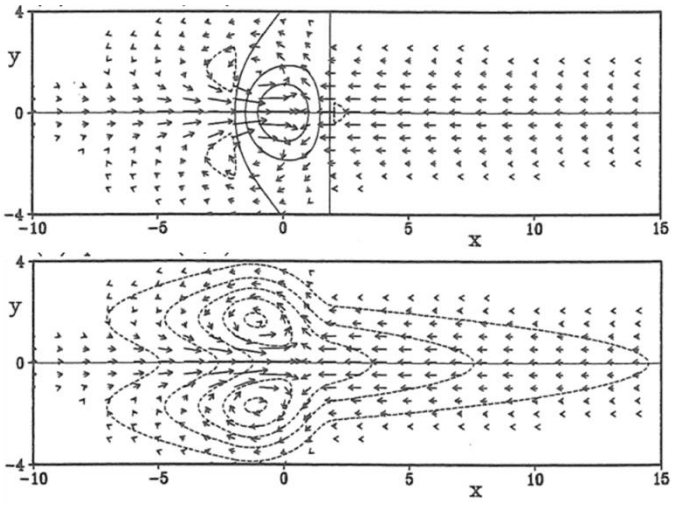

Figure 3.7
Gill's solution for heating symmetric about the equator.
(top) induced vertical motion and circulation at the low level
(bottom) induced surface pressure anomalies and circulation at the low level.

First, we focus on the most basic state, namely the response to the equatorially symmetric heating. Figure 3.7 shows the solution of the Gill model for the symmetric heating. The upward vertical motion basically coincides with the imposed heating field. Gill interpreted this circulation pattern in terms of the propagation of the large-scale equatorial Kelvin and Rossby waves. The low-level easterlies to the east of the heating are due to a Kelvin wave propagation eastward in the presence of the damping. The low-level westerlies to the west of the heating are the result of westward propagation of the damping n=1 Rossby wave. Since Kelvin waves move eastward at a speed roughly three times that of the fastest moving Rossby wave, when a steady state is reached, the damping distance of the Kelvin waves is about three times larger than the damping distance of the Rossby waves. Since induced circulation has a baroclinic structure, circulation at the upper-level shows a reverse direction shown in Figure 3.7.

Then, let's compare Gill's ideal numerical experiment with real atmospheric circulation to interpret its dynamics. The equator-symmetric heating is similar to the case seen in the inter-monsoon season, for example, April (see Figure 3.8).

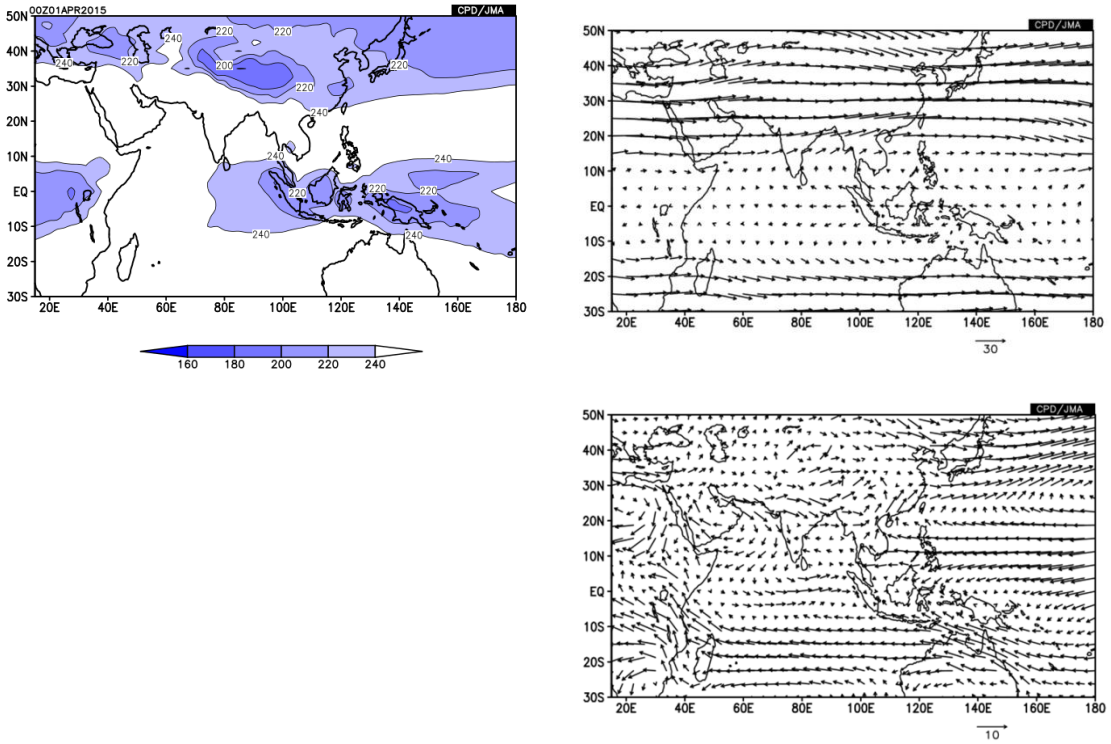

Figure 3.8 Monthly mean OLR (left, unit: W/m^2), wind at 200 hPa (top-right) and wind at 850 hPa level (bottom-right, unit: m/s) for April

Exercise 3.2

Closely compare Figures 3.7 with 3.8, and please identify the cyclonic circulations in Figures 3.8 corresponding to that shown in bottom panel of Figure 3.7.

Figure 3.9 show Gill's solution for the antisymmetric heating. The major ascent and descent regions tend to coincide with imposed heating and cooling, respectively. There is a cyclonic circulation in the heated hemisphere and anticyclonic circulation in the cooled hemisphere at low levels. There is no response to the east of the heat source because of the absence of equatorially symmetric eastward propagating Kelvin waves. Along the equator there are northerly (southerly) winds in the lower (upper) level, which means that mass is transported from the cooling (heating) hemisphere to the heating (cooling) hemisphere in the lower (upper) level.

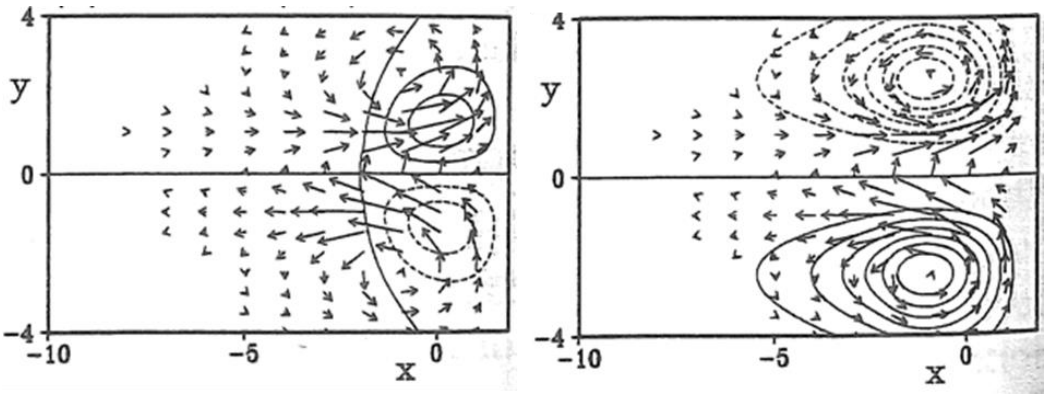

Figure 3.9 Gill's solution for heating asymmetric about the equator.

(left) induced vertical motion and circulation at the low level.

(right) induced surface pressure anomaries and circulation at the low level.

A circulation pattern more relevant to the Asian monsoon may be obtained using a thermal forcing that is the sum of the symmetric and antisymmetric forcing (Figure 3.10). If the equatorial Rossby radius of deformation *Rc* is taken to be 10 degree of latitude, the solution corresponds to a maximum heating at 10N covering 40 degree of latitude. This heat source is similar to the summer monsoon heating in the Bay of Bengal and the Philippines, except that the latter is centered near 15N.

Exercise 3.3

Closely compare Figures 3.6 with 3.10, and please describe similarities seen in both figures.

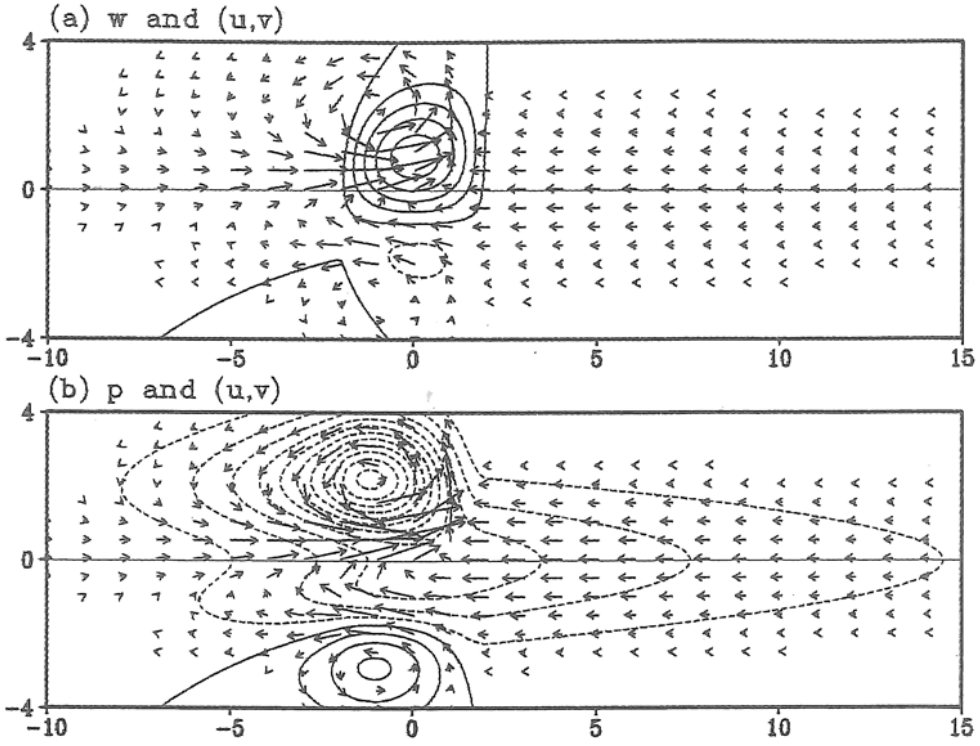

Figure 3.10 Gill's solution for heating asymmetric about the equator which is the sum of the heatings shown in Figure 3.7 and Figure 3.9.
(top) induced vertical motion and circulation at the low level.
(bottom) induced surface pressure anomaries and circulation at the low level.

There is a low-level cyclonic circulation in the heating hemisphere (corresponding to the summer hemisphere) to the west of the heating, due to westward propagation of the long Rossby waves. The flow pattern to the east of the heating region is due to the eastward propagating Kelvin waves. Thus, the winds are easterlies toward the heat source and tend to be parallel to the equator and symmetric about the equator. In the cooling hemisphere (corresponding to the winter hemisphere), the cooling and equatorial warming induced solution shows a weak trough close to the equator and an anticyclonic circulation poleward of this. The entire circulation pattern bears close similarity to the summer circulation in the Indian-Pacific Ocean. Analogous to observations, the dominant component is the Pacific blanch, which consists of easterly winds at the lower troposphere, westerly winds at the upper troposphere, rising motion over the western Pacific, and subsidence over the eastern Pacific. The zonal mean meridional circulation is referred to as the 'Hadley cell'.

Assuming that advection by any basic state may be neglected, the undamping vorticity equation may be written in z-coordinates as (3.1).

$$\frac{\partial \zeta}{\partial t} + \beta v = f\frac{\partial w}{\partial z} \quad (3.1)$$

Scale analysis shows that the thermodynamic equation may be written as:

$$N^2 w = Q \quad (3.2)$$

Consider a region of large-scale, deep convective heating in the equatorial region. Equation (3.2) shows that there is ascent in the region of heating, with adiabatic cooling balancing the diabatic heating. The stretching term in the vorticity equation then implies the tendency to create cyclonic circulations in the lower troposphere and anticyclonic circulation in the upper troposphere. Figure 3.10 is the schematic diagram showing response of the tropical atmosphere to an imposed deep cumulus heating ((a): initial tendency and (b) equilibrium solution).

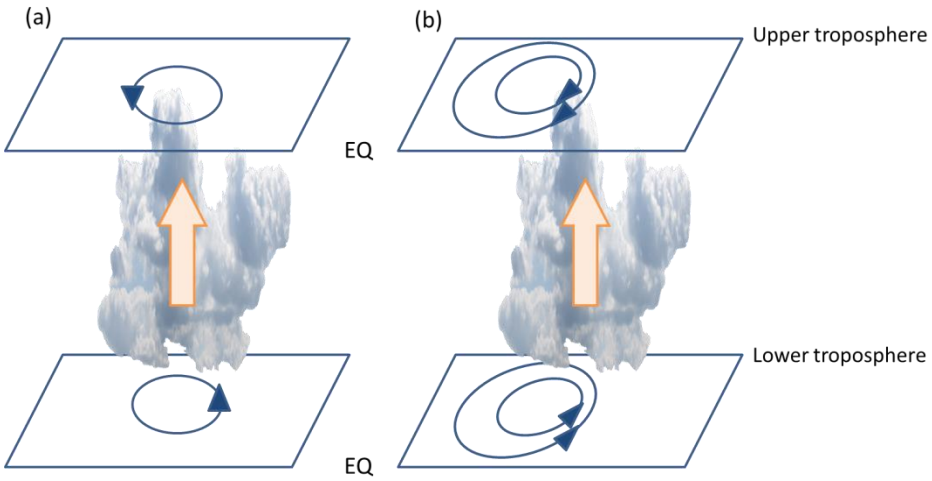

Figure 3.11 The schematic diagram showing response of the tropical atmosphere to an imposed deep cumulus heating ((a): initial tendency and (b) equilibrium solution).

Under the action of the beta-effect, which is described in the vorticity equation, these circulations tend to drift westward just as occurs in Rossby waves. The equilibrium situation is reached when they have drifted to the point where there is a balance in the convective region (3.3).

$$\beta v = f\frac{\partial w}{\partial z} \quad (3.3)$$

This is often referred to as 'Sverdrup balance'. Figure 3.12 shows monthly mean wind field in the upper and lower troposphere superimposed OLR for August and these maps help us interpret the meaning of equation (3.3). For example, in the upper troposphere (left panel of Figure 3.12), the shrinking of vortex tubes (active convection area) is balanced by the advection of larger basic vorticity from higher latitudes (northerly wind component over Southeast Asia).

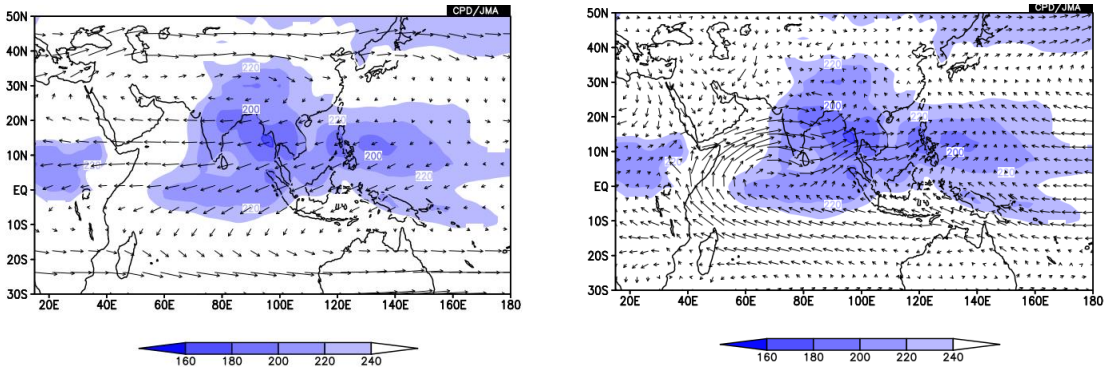

Figure 3.12 Monthly mean OLR (shading, unit: W/m^2) and wind at 200 hPa (left) and 850 hPa level (right) for August.

Combining (3.2) and (3.3) leads to the approximate relationship:

$$\beta v \approx f \frac{\partial}{\partial z}\left(\frac{Q}{N^2}\right) \quad (3.4)$$

This form emphasizes the importance of the vertical distribution of heating.

These vorticity arguments give a perspective on the motions forced by large-scale, deep convective heating that is complementary to that given by the wave approach.

3.4 Cross-equatorial flow in the lower troposphere

The low-level cross-equatorial flow in the western Indian Ocean stands out as the strongest low-level jet on Earth during boreal summer. It has been recognized in early studies of the south-west Indian monsoon that the monsoon flows originate south of the equator (Figure 3.13 (a)). The low-level monsoon airflow is organized into a relatively narrow high-speed trans-equatorial current in the western periphery of the monsoon region. The core is located about 1.5 km above sea level, 200-400 km width, and 1 km in depth and lies about 200 km east of the East African Highland (Figure 3.13 (b)). Equatorially asymmetric thermal forcing leading to a cross-equatorial pressure gradient is an essential driver for cross-equatorial flow (Figure 3.13 (c)).

This cross-equatorial flow, which is now referred to as the Findlater jet or Somalia jet, is an essential component of the Asian monsoon system. It transports moisture from the southern Indian Ocean to south Asia, connects the Mascarene High and Indian monsoon trough, and completes the lower branch of the Hadley cell of the Asian monsoon. The jet stream also drives a strong seasonal cross-equatorial ocean current, the Somali Current. In addition, the along-shore winds induce intense upwelling farther up the coast, resulting in a SST drop of around 3-4C in the western Arabian Sea (Figure 3.13 (d) and (e)).

To understand the basic dynamics of the cross-equatorial flow, let us focus on a large-scale, steady boundary layer flow. The equation governing the vertically averaged boundary flow on an equatorial beta-plane may be written as follows:

$$u\frac{\partial u}{\partial x} + v\frac{\partial u}{\partial y} = -\alpha\frac{\partial p}{\partial x} + fv + \kappa_s u \quad (3.5a)$$

$$u\frac{\partial v}{\partial x} + v\frac{\partial v}{\partial y} = -\alpha\frac{\partial p}{\partial y} - fu + \kappa_s v \quad (3.5\text{b})$$

In (3.5), α is the specific volume of the air and boundary layer friction is represented by a linear drag with κ_s^{-1}being a time constant associated with surface stress and being typically about 2 days.

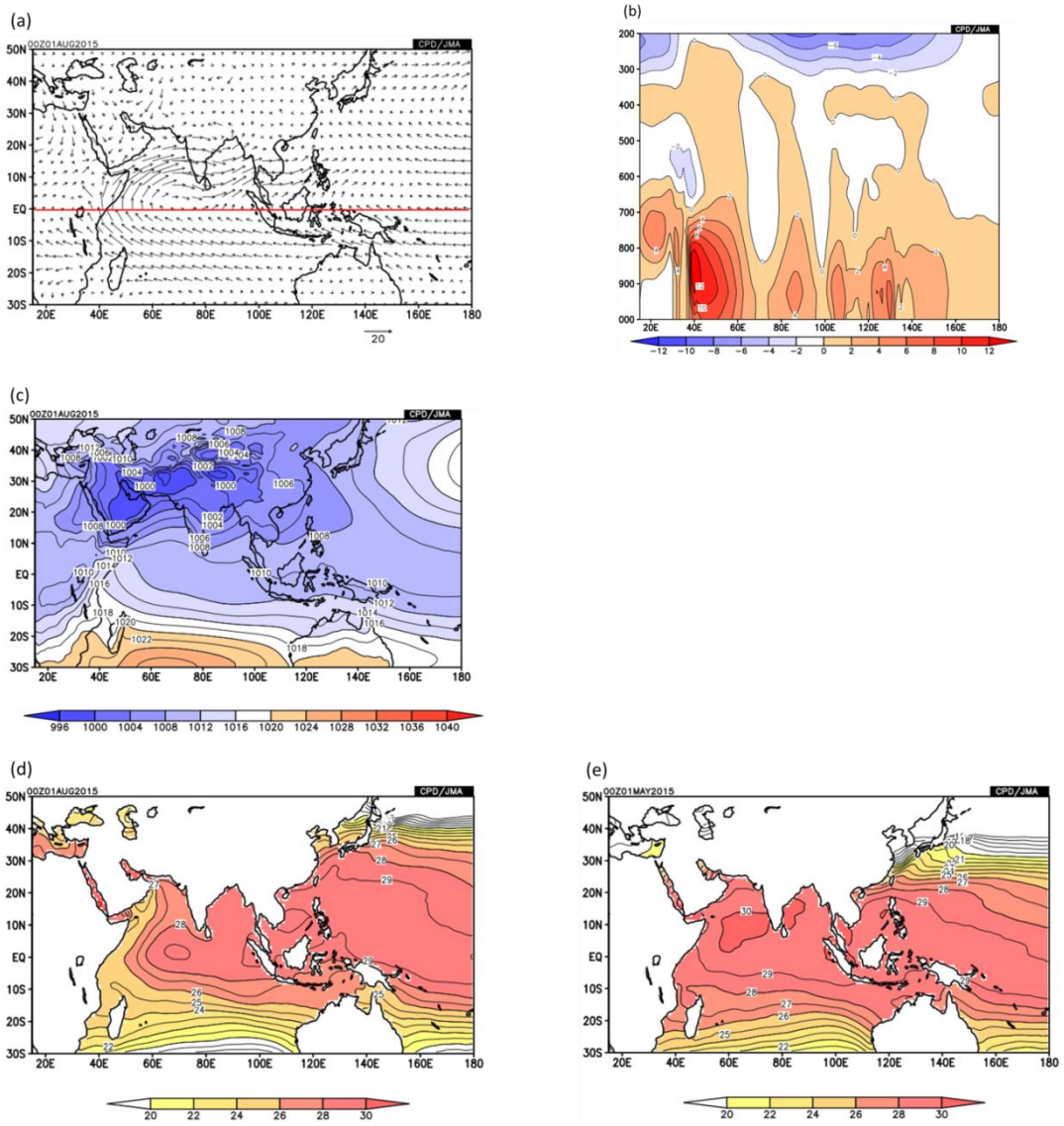

Figure 3.13

(a) Monthly mean wind at 850 hPa level (unit: m/s),

(b) Vertical cross section of monthly mean meridional wind along the equator (unit: m/s),

(c) SLP (unit: hPa),

(d) SST (unit: degree C),

(e) SST for May (unit degree C),

All figures except (e) are for August.

Equatorially asymmetric thermal forcing leading to a cross-equatorial pressure gradient is an essential driver for cross-equatorial flow. Consider now constant meridional pressure gradient extending from wintertime southern subtropics to the low pressure over the heated northern subtropics. At the equator, the Coriolis force vanishes so that if the inertial (advective) terms are negligible then $v = \kappa_s^{-1}\,\alpha\frac{\partial p}{\partial y}$ and the flow is directly across the isobars toward low pressure. For a strong cross-equatorial flow, however, the advective accelerations in the near-equatorial balance of force are essential. If the frictional terms are neglected an inertial regime exists with the left hand side of (3.5a) balanced by the pressure gradient force. Thus the zonal momentum equation (3.5a) at the equator yields a flow that is directly across the equator, namely $v = -\alpha\frac{\partial p/\partial x}{\partial u/\partial y}$ and $u(0) = 0.$ This indicates that zonal pressure differences are essential for a strong cross-equatorial flow such as the Somalia jet.

3.5 The Tibetan High and the tropical easterly jet

In the upper troposphere such as 200hPa level, a prominent circulation system of the Asian summer monsoon is the planetary-scale high-pressure system and associated anti-cyclonic circulation. This system is centered over the Tibetan Plateau and is often referred to as the Tibetan High or south Asian High. The clockwise flow (anticyclone) around the Tibetan High contains an easterly jet stream in its southern flank called the tropical easterly jet. Pronounced cross-equatorial flow in the Indian Ocean is a major component of the upper level branch of the Hadley cell (Figure 3.14). It is notable that the zonal wind component of the easterly jet, although located in the deep tropics, is nearly in geostrophic balance with the meridional pressure gradient force. Scale analysis shows that this is because the Rossby number V/fL for the jet is small, where *L* is the long zonal length scale for this jet and *V* is a typical meridional wind.

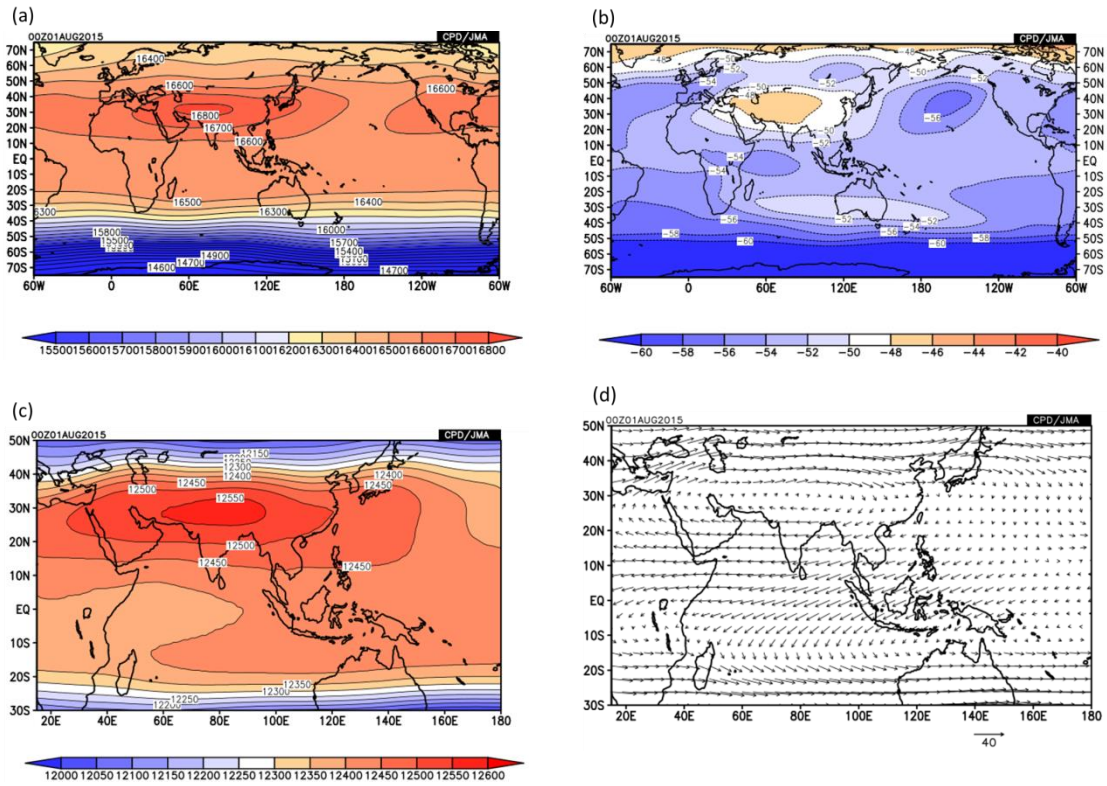

Figure 3.14

(a) Monthly mean geopotential height at 100 hPa level (unit: m),

(b) Monthly mean temperature at 200 hPa level (unit: degree C),

(c) Monthly mean geopotential height at 200 hPa level (unit: m),

and (d) Monthly mean wind at 200 hPa level (unit: m/s) for August.

The formation of the Tibetan High is associated with the strong summertime continental heating and the latent heat release associated with the Asian monsoon. The formation and maintenance of the Tibetan High and the upper tropospheric circulation are primarily attributed to the diabatic heating processes associated with deep convective rainfall in south-east Asia and the western North Pacific and also to the sensible and convective heating over the elevated Tibetan High. Above and to the west of the Plateau the cyclone at low levels and the anticyclone at upper levels are associated hydrostatically with a warm troposphere that has spread westward from the heating region as a long Rossby wave. The Plateau itself acts as an elevated heat source in summer. In particular, the strong surface sensible heat flux makes the boundary layer very unstable and produces strong near-surface convergence and upper level divergence/negative vorticity. As a result, the Tibetan High has a warm and moist core over the Plateau. The mean upper tropospheric temperature over south Asia and the Tibetan Plateau is the highest on the planet (check again Figure 3.14

(b)). This remarkable warmth is directly associated with the intensity of the high pressure in the upper troposphere.

Over the Tibetan Plateau, the local mean temperature is more than 5 degrees C higher than at the equator at the same longitude (see again Figure 3.14 (b)). This reversed poleward temperature gradient is consistent with a strong easterly thermal wind and the existence of the upper level easterly jet. When thinking about vertical circulation associated with the easterly jet, it is of interest to consider an alternative partition of the wind to the rotational and divergent split. The quasi-geostrophic version of the zonal momentum equation may be written as (3.6).

$$\frac{du_g}{dt} = f\left(v_g + v_a\right) - \frac{1}{\rho}\frac{\partial p}{\partial x} = f v_a \quad (3.6)$$

Here the meridional wind component has been decomposed into a geostrophic (v_g) and ageostrophic (v_a) component (i.e., $v = v_g + v_a$). Evidently, on the north side of the entrance region of the easterly jet (the monsoon trough from the Bay of Bengal to the Philippine Sea), a parcel moving through the jet will experience an increase in easterly wind speed $(du_g/dt < 0)$. Equation (3.6) implies that in this entrance region of the jet there must be a northerly ageostrophic flow, and consequently upper level divergence and mid-level ascent over the south-east Asian monsoon trough region (see again equation (3.3)). To consider the wind field divided into the rotational and divergent component, we introduce a stream function and a velocity potential. The rotational component of geostrophic winds flows parallel to the contours of stream function and larger stream functions are 90 degree to the right of the direction toward which the winds are blowing. The divergent component of wind flows parallel to the gradient of velocity potential.

Exercise 3.4

Please answer the following questions by referring to Figures 3.15 in the next page.

(a) Where is the entrance region of the easterly jet?

(b) Which direction does ageostrophic wind (i.e. divergent component) flow in the entrance region of the easterly jet?

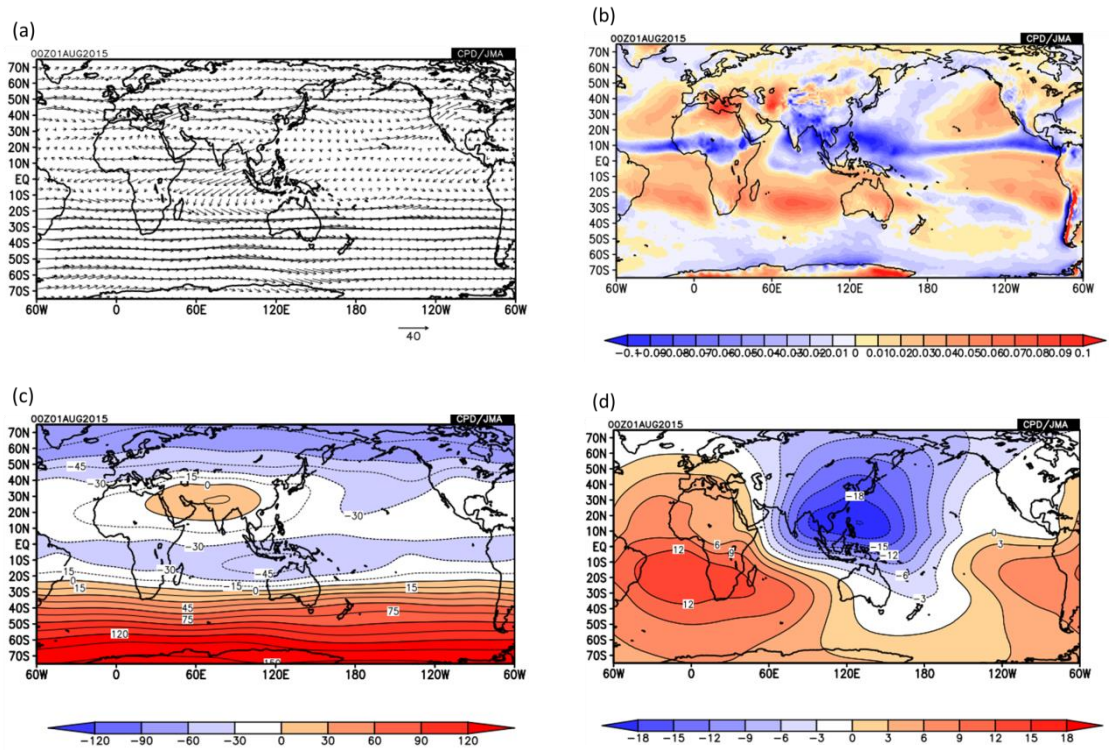

Figure 3.15

(a) Monthly mean wind at 200 hPa level (unit: m/s),

(b) Monthly mean vertical pressure velocity at 500 hPa level (unit: Pa/s),

(c) Monthly mean stream function at 200 hPa level (unit: 10^6 m^2/s),

(d) Monthly mean velocity potential at 200 hPa level (unit: 10^6 m^2/s)

for August.

The ascent along with the upper level northerly ageostrophic flow forms a secondary circulation which consists of a southerly flow crossing the equator and a sinking motion just south of the equator. This secondary circulation is an enhancement of the monsoon Hadley cell and consistent with the ascent in the monsoon trough. A particular point that is noteworthy is that the south-east Asian heating contributes to the formation and maintenance of the Tibetan High and the upper tropospheric easterly jet. On the other hand, the upper level easterly jet has an associated secondary circulation, in turn, favors development of deep convection.

In the lower troposphere, the south-easterly trades associated with the North Pacific subtropical anticyclone meet the south-westerly monsoon, forming a confluence zone - the monsoon trough over the Philippines.

Thus, the heating-induces, large-scale circulation is in favor of the maintenance of heavy monsoon rains

in south-east Asia where low-level flows converge and upper level flows diverge. The above argument implies that the dynamical forcing provided by the heating-induced, large-scale circulation feeds back positively to reinforce the strength of the convection in the south-east Asian monsoon trough. Arguably, this positive feedback may play a critical role in selecting the preferred location for the monsoon trough and heavy monsoon rainfall.

It should be noted that the Tibetan High and easterly jet are not solely due to the effect of the south-east Asian monsoon rainfall. The Tibetan Plateau is also a major factor determining the character of the Tibetan High and easterly jet. The location of the elevated heat source to the north of 25N over the Plateau is perhaps sufficiently strong to provide an anchor for the central location of the Tibetan High, which in turn, sets the location of the tropical easterly jet and the ascent region influenced by the secondary circulation in the jet entrance region. The latter favor heavy rains establishing in the Asian monsoon trough region. Thus, the Tibetan Plateau may make a considerable contribution in determining the location of the whole monsoon structure.

On the other hand, North Africa is located in the exit region of the northern side of the easterly jet where the easterly decreases in intensity, resulting in upper level southerly ageostrophic winds and convergence on the northward side. The resultant secondary circulation is consistent with subsidence over the North African region on the poleward side of the poleward side of the easterly jet, which may restrict the northward extension of the Sahel monsoon rainfall and confine the rain belt to the coastal zone of North Africa.

3.6 Termination of summer monsoon and winter monsoon

Please recall that the fundamental forcing of the atmospheric circulation and climate ultimately relates to the radiation budget of the planet and that the dominant annual cycle forcing is the change in distribution of incoming solar radiation due to the orbit of the Earth around the sun (see again Figure 3.1). Responding the change in the radiation forcing, the cross-equatorial pressure gradient diminishes around October and November, and then, changes its direction around December or January (Figure 3.16). This brings the termination of summer (southwest) monsoon and inter-monsoon season, then the onset of winter (northeast) monsoon.

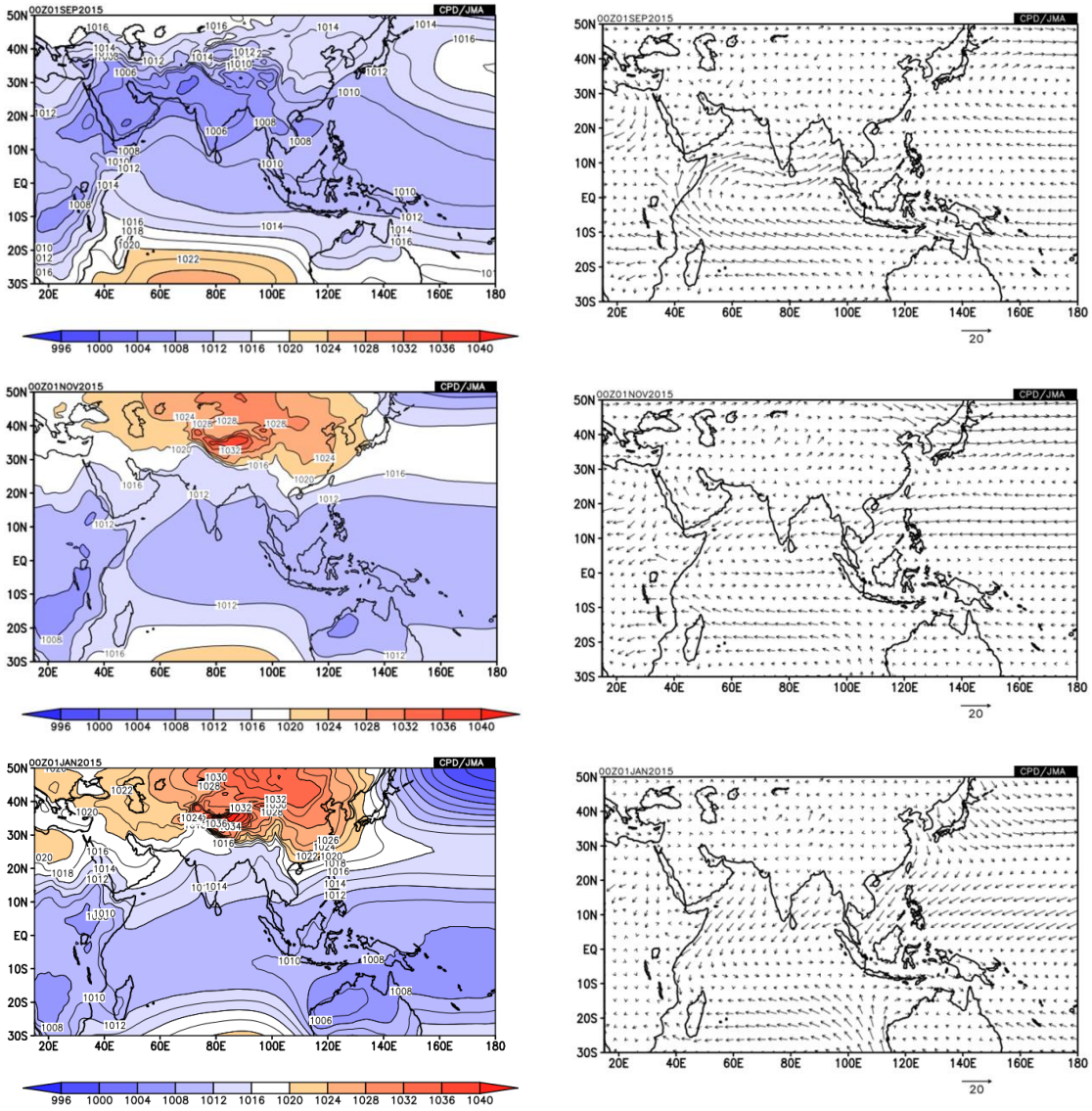

Figure 3.16 Monthly mean sea level pressure (SLP) (left, unit: hPa) and wind at 850 hPa level (right, unit: m/s) for September (top), November (middle) and January (bottom).

However, the boreal winter present a very different structure. The temperature gradients in the southern hemisphere never reverse. Although Australia is a large continent, the heating is not elevated as it is over the Himalayas. Thus, the major heating remains close to the north coast of the continent and close to the equator. As a result, a warmer area is restricted within a much smaller section of the globe (northeast Australia) (Figure 3.17). Though, there are still strong cross-equatorial pressure gradients that drive boreal winter monsoon. There gradients, not as large as those occurring in the boreal summer, are the result of the intense radiational cooling over north Asia during winter (this is indicated by the top panel of Figure 3.2).

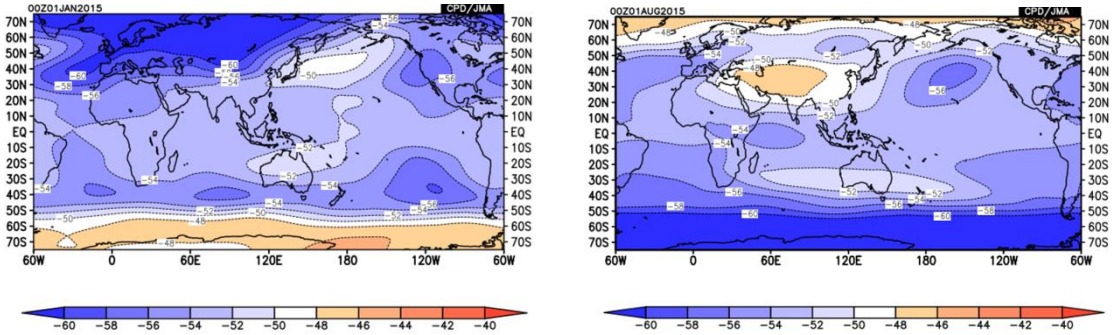

Figure 3.17 Monthly mean air temperature at 200 hPa for January (left) and August (right) (unit: degree C).

4. Intraseasonal variabilities of monsoon and monitoring

While the defining variability of a monsoon system is its seasonal character, its variability about its typical seasonal evolution (reviewed in the previous chapter) is often most of interest and importance. In the case of the Asian and Australian summer monsoons, their intraseasonal character is especially prominent and unique. This intraseasonal variability has two important features. In this chapter, we review the characteristics of main intraseasonal variabilities and then consider how to monitor them. Examples of monitoring measures used by the Tokyo Climate Center (TCC) are also introduced.

4.1 Madden-Julian Oscillation (MJO)

Despite over a century of interest and study of the interannual component of the Asian monsoon, the prominence of an organized intraseasonal component has only been recognized for about the last four decades. One of the first steps in this recognition came in the early 1970s with the discovery of an intraseasonal 'oscillation' in the tropics that has since been named the Madden-Julian Oscillation (MJO) after its discoverers. Figure 4.1 shows OLR anomalies in association with MJO and this illustrates eastward propagation with relatively long period (say 30-60 or 30-90 days) and equatorially trapped character. It can be seen that the MJO has a global scale with wind and rainfall anomalies being primarily characterized by zonal wavenumber 1. This characteristic is modulated by the relatively warmer (cooler) eastern (western) hemisphere background state. For example, over the Indian and western Pacific Ocean, there is evidence of considerable interaction between the wind and rainfall anomalies. In these regions, where the coupling between the convection and warm surface waters is strong, the oscillation propagates rather slowly, about 5-10 m/s. On the other hand, once disturbances reach the vicinity of the Date Line, and thus cooler eastern Pacific Ocean equatorial waters, the convection tends to subside and propagate south-eastward into the

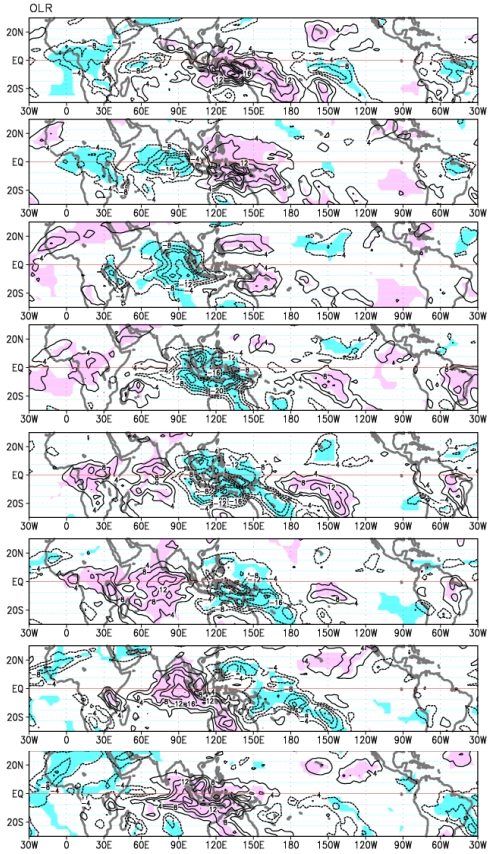

Figure 4.1 Composite of OLR anomalies for each phase of MJO. Cold (warm) color indicates enhanced (suppressed) convective activity.

South Pacific convergence zone (SPCZ). Beyond the Date Line, the disturbance if primarily evident only in the wind field with characteristics similar to a dry Kelvin wave with a phase speed of about 15-20 m/s or greater.

Exercise 4.1

Referring to the above text, convert the unit of a typical phase speed of MJO from [m/s] to [degree (longitude)/day] along the equator for below both regions.

(1) Over the Indian and western Pacific Ocean

(2) Beyond the Date Line

Exercise 4.2

Considering its characteristics, which of the followings is thought to be the most preferable to monitor the MJO?

(a) Time-latitude cross section of OLR anomalies along a specific longitude

(b) Time-longitude cross section of OLR anomalies along the equator

(c) Time-altitude cross section of zonal wind anomalies at a specific point

(d) Time-latitude cross section of zonal wind anomalies at 850 hPa level along a specific longitude

Associated with the enhanced rainfall (i.e. heating) over the Maritime Continent, there are upper level cyclonic (anticyclonic) circulation anomalies to the north-east and south-east (north-west and south-west) centered at latitudes of about 20 degree (Figure 4.2). These circulation anomalies are consistent with the circulation that is expected in association with a near-equatorial tropospheric heating anomaly. One of the important manifestations of these tropical heating and subtropical stream function anomalies is that they act as Rossby wave sources for mid-latitude variability. That is, the MJO could influence climate conditions not only of the tropics but of the extra-tropics, and given this feature and its relatively longer period, it could also bring a predictability of monthly or seasonal time scale. This is why TCC routinely monitors the MJO with great interest.

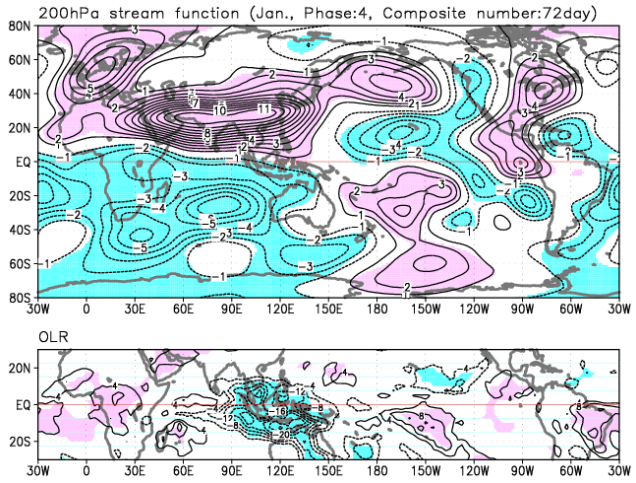

Figure 4.2 Composite of 200-hPa stream function (top) and OLR (bottom) anomalies.

Cold (warm) color indicates negative (positive) anomalies.

TCC monitors the MJO mainly by two measures. One is the MJO Monitoring Indices introduce by Wheeler and Hendon (2004). This measure is based on multivariate EOF analysis of daily 850 hPa zonal wind, 200 hPa zonal wind and OLR (15ºS-15ºN) for the period of 1981 - 2010. To extract an MJO component from the 850 hPa zonal wind, 200 hPa zonal wind and OLR, the annual cycle and components of interannual variability (including ENSO) are removed first. Two principal component time series from multivariate EOF of the MJO components are defined as RMM1 and RMM2. Two-dimensional phase space is defined by RMM1 and RMM2. The spatial structures of RMM1 and RMM2 are rotated with reference to the structures of Wheeler and Hendon (2004) due to the phase displacement of the EOF vectors. Then by projecting the current zonal winds and OLR distribution on these principal components, the current values of RMM1 and RMM2 are derived. In the MJO monitoring TCC plots these current RMM values on the two-dimensional phase space defined by RMM1 and RMM2 (Figure 4.3). This phase space divides the equatorial zones into 8 phases indicating the position of active phase of the MJO and the distance from the center of phase space and the plotted point indicates the amplitude of the MJO. In association with the eastward propagation of MJO, trajectory of RMM1 and RMM2 draws anti-clockwise circles in the phase space. Figure 4.3 is the example for June 2015. This diagram indicates that the active phase of MJO propagated over the Indian Ocean to the western Pacific with large amplitude.

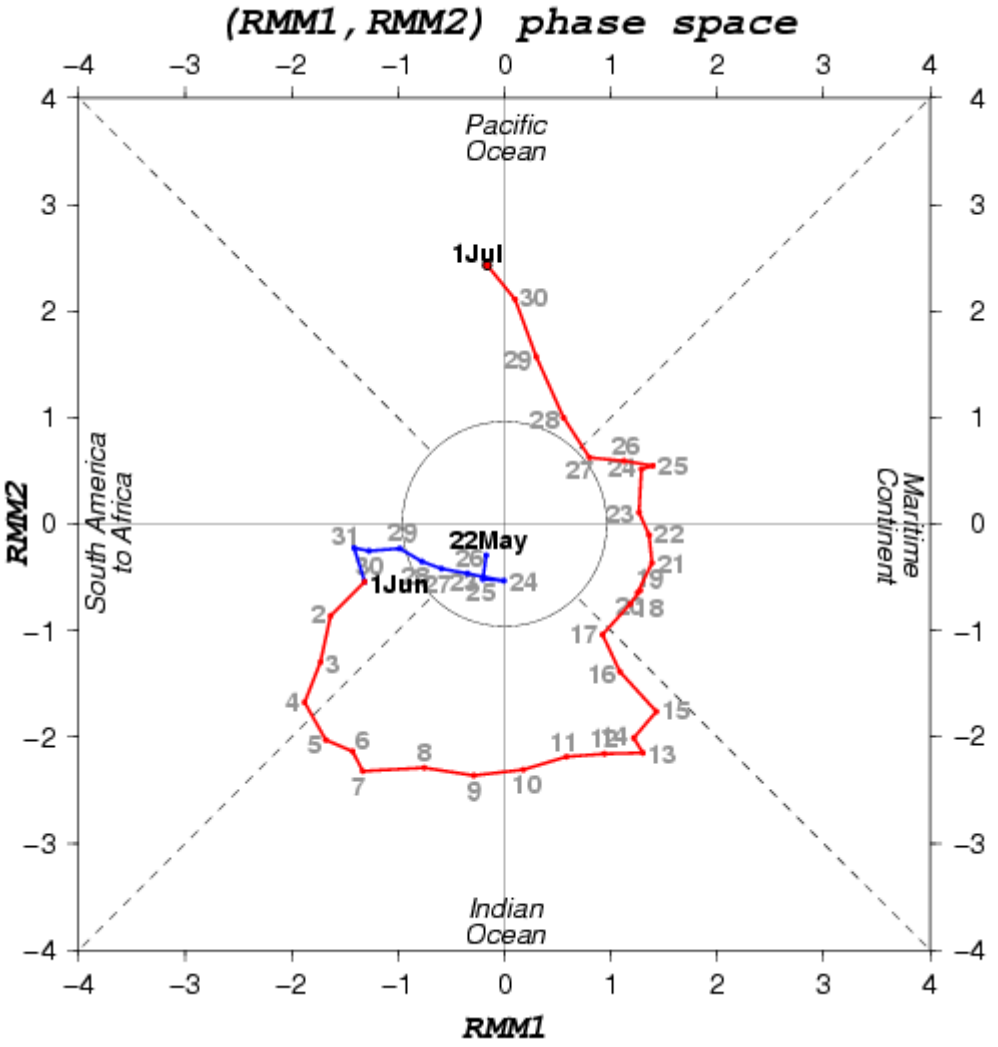

Figure 4.3 MJO phase monitor based on multivariate EOF analysis.

Example for June 2015.

Another measurement is the time-longitude cross section of anomalies of OLR, upper-level velocity potential and lower-level zonal winds along the equator. Taking into account the characteristics of the MJO (eastward propagation, relatively long period (30-60 or 30-90 days) and equatorially trapped), these cross-section maps are expected to quickly detect and monitor the MJO more easier manner than the MJO Monitoring Indices introduce by Wheeler and Hendon (2004). Figures 4.4 are the time-longitude cross section of anomalies of upper-level velocity potential (left), OLR (middle) and lower-level zonal winds (right) along the equator from March to August 2015.

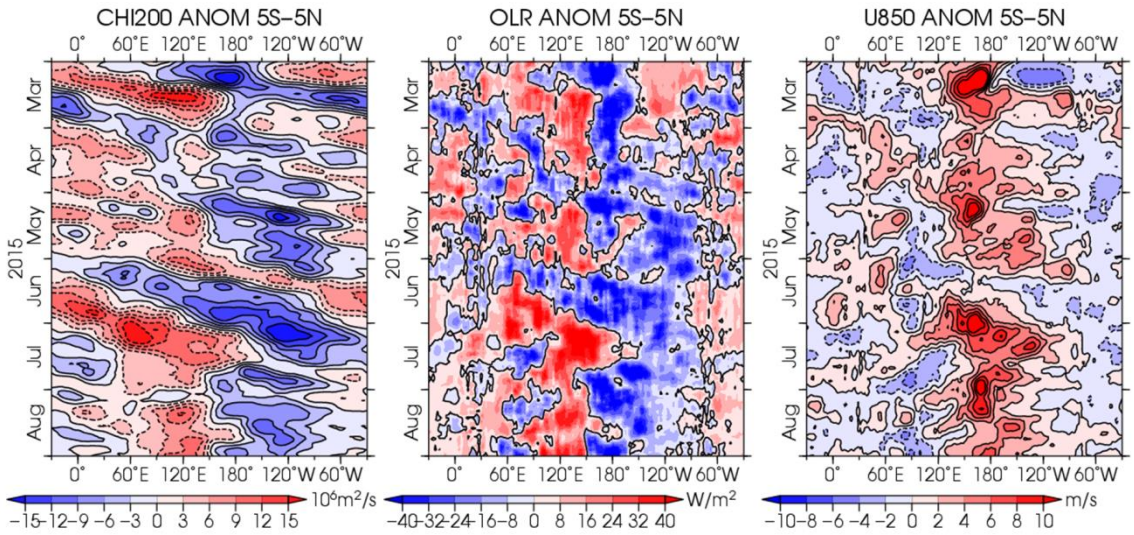

Figure 4.4 The time-longitude cross section of anomalies along the equator from March to August 2015. (left) upper-level velocity potential, (middle) OLR and (right) lower-level zonal winds. 7-day running mean is done to cancel a high-frequency noise.

Let's focus on the period June 2015. These figures clearly depict that negative anomalies of upper-level velocity potential and OLR (both indicate enhanced convective activity) moved eastward from Indian Ocean to the Pacific with one-month or longer period, and this is consistent with Figure 4.3. In monitoring the MJO, we need to pay attention to westerly wind anomaly which moves on the behind of (i.e. west of) active convection. In the case of June 2015, a strong westerly wind anomaly followed the enhanced convection. This is because in some cases, a strong westerly anomaly associated with the MJO could serve as a "westerly burst" to trigger El Niño event.

The details and latest of products introduced here, and other related products are available from the TCC website.

http://ds.data.jma.go.jp/tcc/tcc/products/clisys/mjo/moni_mjo.html

4.2 Boreal Summer Intraseasonal Oscillation (BSISO)

Beginning around the mid to late 1970s, a number of studies began to identify intraseasonal fluctuations with periods of 40-50 days associated with the Asian summer monsoon. A typical boreal summer intraseasonal oscillation (BSISO) brings positive rainfall anomalies in the western and central Indian Ocean in conjunction with negative anomalies over a region extending between India and the western equatorial Pacific. This system then appears to propagate both an eastward and northward fashion. Examination of the near-equatorial region alone gives the impression of MJO-like phenomenon, although more confined in longitude. On the other hand, examination of a give longitude sector anywhere between 80 to 130E gives the impression of a northward propagating phenomenon. These variations largely account for what are often referred to as "active" and "break" periods of the monsoon.

It is also important to point out that there is a fair bit of variability even within the monsoon season where considering the nature of BSISO events and the influence of the background state. For example, Figure 4.5 illustrates how the typical pattern of intraseasonal variance is modified over the course of the monsoon season. This seasonal variation was shown to be consistent with the seasonal march of the warmest SSTs, which begin to develop in the northern Indian Ocean in the early monsoon period and eventually are found around south-east Asia and the northwestern tropical Pacific in the later part of the summer.

With the above seasonal modulation in mind, Kemball-Cook and Wang (2001) produced a schematic of the synoptic evolution of an intraseasonal oscillation event. This diagram is shown in Figure 4.6. It illustrates a mixture of the underlying wave characteristics, and their propagating features.

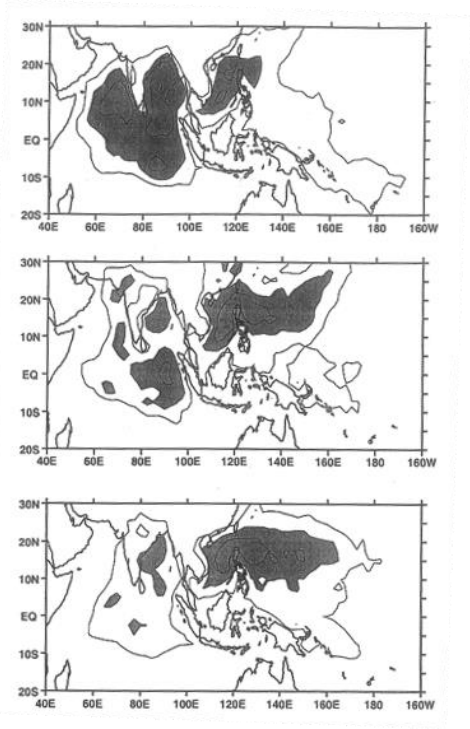

Figure 4.5

Seasonal variation of 10-100-day filtered ORL variance.

First contour is drawn at 500 $(W/m^2)^2$ and regions where the OLR variances > 750 $(W/m^2)^2$ are shaded.

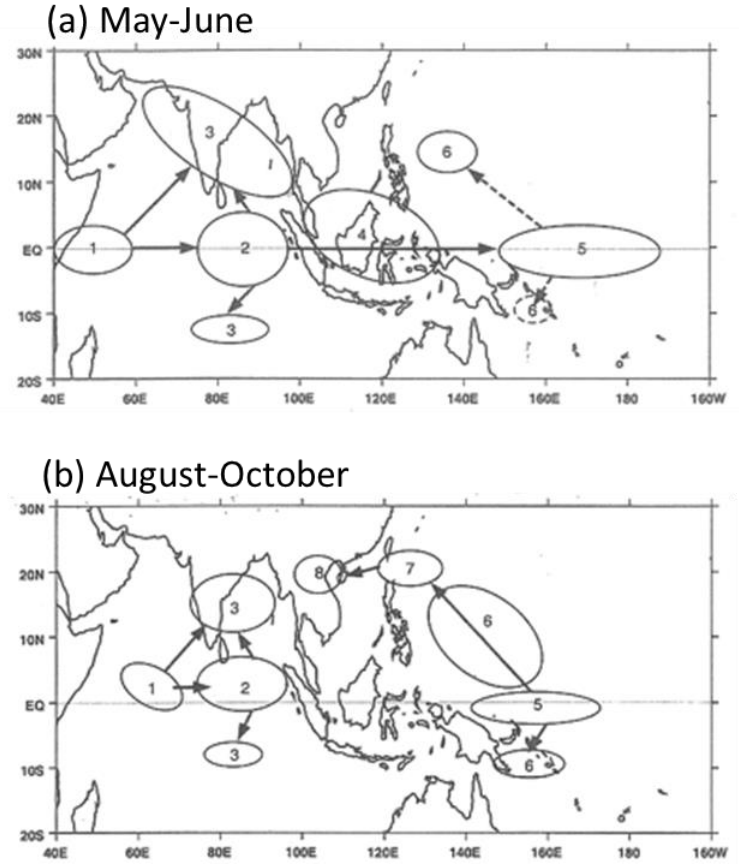

Figure 4.6 Boreal summer intraseasonal oscillation convection life cycle for (a) May-June and (b) August-October.

Ovals indicate convection, with numbers indicating the evolution of the anomaly. Horizontal arrows indicate eastward propagation of convection along or near the equator. Vertical/slanted arrows indicate poleward propagation of convection due to emanation of Rossby waves from equatorial convection.

For both the early and late monsoon season, there is what can be considered an initiation phase in the equatorial Indian Ocean, an eastward propagating component, and a recurrent emission of Rossby waves. For the initiation phase, the main difference between early and late summer, is that during the late summer there is an eastward displacement of the location of the initiation phase. For the eastward propagating component, the main difference is that in the late summer, the propagation appears to be somewhat discontinuous and 'jumps' across the Maritime Continent. In addition, there is less latitudinal symmetry in late summer, as warm moist surface conditions have moved mostly to the north of the equator.

The off-equatorial disturbances shown in Figure 4.6 are associated with the emanation of Rossby waves from the near-equatorial convection anomaly. It is this feature that makes the propagating characteristics of

the BSISO particularly complex. These disturbances are associated with three directions of propagation. Considered in isolation, they have an inherent westward propagation. This accounts for some aspects of the westward propagating variability that is found, particularly in the latter part of the summer, in the south-east Asian sector/western North Pacific Ocean. On the other hand, the emanation of these Rossby waves occurs from a very large-scale, eastward moving, near-equatorial convective anomaly. Finally, there are physical processes that promote northward propagation of these Rossby wave disturbances, that largely accounts for the appearance of the eastward propagating, northwest-southeast tilted, large-scale 'rain band'.

Taking into account its importance on intraseasonal variability of summer monsoon and its northward-propagating feature, TCC routinely monitors BSISO, for example, by using latitude-time cross-section of OLR. Figure 4.7 is an example that shows the latitude-time cross-section of OLR from April to September 2010. In order to eliminate the 'noise' from very short-period fluctuations and focus on intraseasonal timescales, we take 5-day running mean of daily OLR data. Looking at longitudes of the Bay of Bengal (top panel), we can easily find two events that convection inferred from low OLR propagated northward in mid-May and early June. The former event could bring the onset of the summer monsoon of that year and the latter could bring the "active" periods of the monsoon.

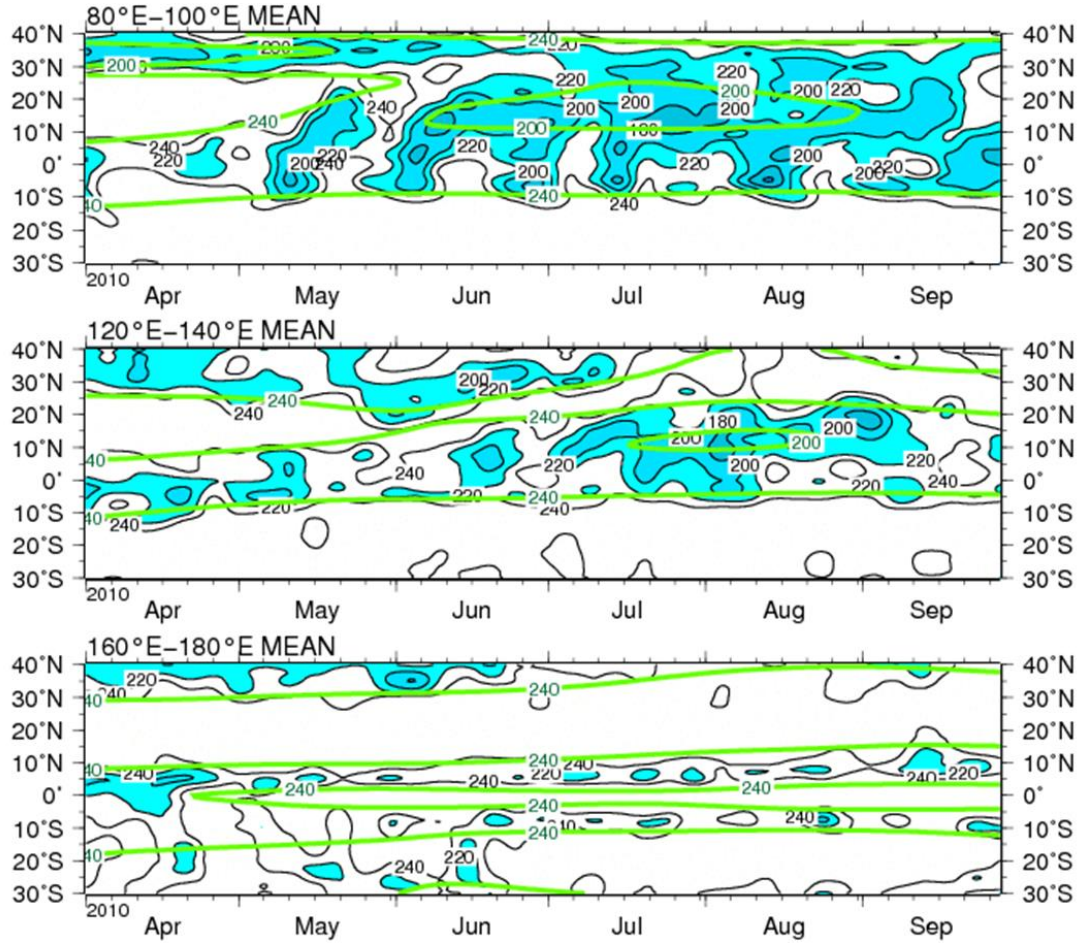

Figure 4.7 Latitude-time cross section of five-day running mean OLR for 2010.

The black lines show OLR at interval of 20 W/m^2 and the green lines indicate its climatological normal of 200 and 240 W/m^2.

The various kinds of charts (including this example) and monitoring indices are available from the web page below.

http://ds.data.jma.go.jp/tcc/tcc/products/clisys/acmi.html

References

Gill, A. E., 1980: Some simple solution for heat-induced tropical circulation. *Quart. J. Roy. Meteorol. Soc.*, **106**, 447-462.

Kemball-Cook, S. and B. Wang, 2001: Equatorial waves and air-sea interaction in the Boreal summer intraseasonal oscillation. *J. Climate*, **14**, 2923-2942.

Li, C. and M. Yanai, 1996: The onset and interannual variability of the Asian summer monsoon in relation to land-sea thermal contrast. *J. Climate*, **9**, 358-375.

Wallace, J M., and P. V. Hobbs, 2006: *Atmospheric science: an introductory survey.* Vol. 92. Academic press.

Wang, B. 2006: *The Asian monsoon.* Springer Science & Business Media.

Wheeler, M. C. and H. H. Hendon, 2004: An all-season real-time multivariate MJO index: Development of an index for monitoring and prediction. *Mon. Wea. Rev.*, **132**, 1917-1932.

SRI LANKA JOURNAL OF METEOROLOGY
Contents
Vol. II, September 2017
Special Issue
Lectures on Tropical Meteorology

Articles: